RESEARCH

AP5Z1 affects hepatocellular carcinoma growth and autophagy by regulating PTEN ubiquitination and modulating the PI3K/Akt/mTOR pathway

Zhipeng Quan[1,2,3†], Bo Peng[1,2,3†], Kai Hu[3,4], Lixing Liang[3,4], Mingjiang Liu[1,2,3], Lijuan Liao[1,2,3], Shilian Chen[1,2,3], Jing Qin[3,4], Songqing He[1,2,3*] and Zeyuan Li[1,2,3*]

Abstract

Background Hepatocellular carcinoma (HCC) is a leading cause of cancer death worldwide, with high incidence and mortality rates, and the number of cases is expected to increase by 2030. Understanding the molecular mechanisms of HCC and identifying new therapeutic targets and biomarkers for HCC are crucial.

Methods In this study, we examined adaptor-related protein complex 5 subunit ζ1 (*AP5Z1*) expression in liver cancer and nearby noncancerous tissues to explore its effects on HCC cell growth, death, and autophagy. The functional and molecular mechanisms of *AP5Z1* were studied using clinical sample analysis, Western blot (WB), immunohistochemistry (IHC), quantitative reverse-transcription polymerase chain reaction (qRT–PCR), coimmunoprecipitation (Co-IP), cell proliferation assays, flow cytometry (FCM), autophagy assays, electron microscopy, mass spectrometry (MS), transcriptome analysis, and animal model experiments.

Results *AP5Z1* expression was notably higher in HCC tissues than in normal tissues and was linked to a poor prognosis. The results of both in vitro and in vivo studies revealed that *AP5Z1* promoted HCC cell growth and reduced apoptosis. In addition, *AP5Z1* regulates cellular autophagy by ubiquitinating the phosphatase and tensin homolog (PTEN) protein and modulating the phosphoinositide 3-kinase (PI3K)/protein kinase B (Akt)/mammalian target of rapamycin (mTOR) pathway.

Conclusions *AP5Z1* influences autophagy and apoptosis in HCC cells by interacting with PTEN to modulate the PI3K/Akt/mTOR pathway. This gene might promote PTEN ubiquitination and degradation by recruiting tripartite motif-containing protein 21 (TRIM21), making it a potential biomarker for diagnosing and predicting the outcome of HCC as well as a target for new treatment strategies.

†Zhipeng Quan and Bo Peng contributed equally to this work.

*Correspondence:
Songqing He
dr_hesongqing@163.com
Zeyuan Li
lizeyuan03@126.com

Full list of author information is available at the end of the article

Background

Globally, cancer is one of the leading causes of death, with hepatocellular carcinoma (HCC) ranking as the sixth most common form and a major cause of cancer-related death [1]. Researchers have constructed age/period/cohort models using Nordpred software (kreftregisteret.no) to predict new primary HCC cases through 2030 and found that new cases and rates are projected to increase in both men and women [2]. Therefore, in-depth research and discussion on the fundamental causes and molecular regulatory mechanisms of HCC must be conducted.

Recent research has shown that HCCs are associated with abnormalities in the intrinsic biological processes of cells, including aberrant nuclear–exosome transport [3], changes in cell autophagy and changes in immune cell subsets [4–6]. HCC has been treated multimodally for many years, but the prognosis and survival rates have not improved significantly. Therefore, the pathogenesis of HCC requires further study, and efforts to identify potential biomarkers and new therapeutic targets are needed.

Adaptor protein complex (AP) family members are heterotetramers; their main function is to select proteins for inclusion in transport vesicles [7]. Four family members were identified early [8]. AP-5, a more recently discovered member of the family, participates in late nuclear–exosome material transport, including transport and sorting of the important HCC molecular marker Golgi membrane protein 1 (*GOLM1*) within cells [9]. AP family members are reportedly associated with cancer; for example, depletion of the AP-1 subunit γ1 (*AP1G1*) adaptin significantly suppresses breast cancer (BC) [10]. A correlation exists between AP3 subunit σ1 (*AP3S1*) and immunosuppressive tumour microenvironments (TMEs) in pancancer cells [11]; knockdown (KD) of *AP3S1* regulates the migration and invasion of ovarian cancer (OC) cells [12]. AP2 subunit μ1 (*AP2M1*) expression levels were found to be much higher in HCC cells than in matched normal liver cells [13]. Cell spread, migration, and matrix degradation are regulated by the AP-2 complex subunit 2-adaptin in U2OS osteosarcoma cells [14]. These reports suggest that members of the AP family play major roles in tumour development and tumorigenesis. Mutations in the *AP5Z1* gene, which encodes the AP-5 subunit ζ, cause spastic paraplegia and other neurological issues [15, 16]. However, whether AP-5 plays a role in tumour regulation is uncertain.

In this study, we analysed *AP5Z1* expression in HCC and adjacent noncancerous tissues via loss- and gain-of-function approaches to investigate the impact of this gene on the progression of HCC. We found that AP5Z1 functions as an oncogene in HCC and has potential as a therapeutic target or biomarker for HCC patients.

Methods

Clinical samples

Patients with HCC at the First Affiliated Hospital of Guangxi Medical University (GMU; Nanning, China) provided informed consent, and we collected clinical samples from them with approval from the hospital's Ethics Committee. To preserve fresh samples for long-term storage, we froze them in liquid nitrogen.

Cell culture

We sourced the human HCC cell lines MHCC-97 H, HUH-7, SUN-182, SUN-449, and LM3; the normal liver cell line MIHA; and renal epithelial cells (ECs; 293T) from the American Type Culture Collection (ATCC; Manassas, VA, USA). SUN-182, SUN-449, and MIHA cells were grown in Roswell Park Memorial Institute (RPMI) 1640 medium (GIBCO [Thermo Fisher Scientific, Waltham, MA, USA]), while MHCC-97 H, HUH-7, LM3, and 293T cells were cultured in Dulbecco's modified Eagle's medium (DMEM; Gibco). The cells were cultivated under the specified conditions per the instructions of the ATCC.

Cell transfection

Vectors for gene KD or overexpression (OE) and their corresponding negative-control (NC) vectors were purchased from IGE Biotechnology Co., Ltd. (Guangzhou, China). We cotransfected these vectors into HEK293T cells using packaging plasmids (psPAX2 and pMD2.G). Forty-eight to 72 h after transfection, the viral supernatant was collected, mixed with lentiviral concentrate, and left to stand overnight, after which HitransG A (Shanghai JiKai Gene Chemical Technology, Ltd., Shanghai, China) was added to enhance infection. Short interfering ribonucleic acids (siRNAs) for TRIM21 KD were synthesized by Hysigen, Inc. (Sugar Land, TX, USA); their sequences are listed in Supplementary Table 1. Using Lipofectamine 3000 (Invitrogen [Thermo Fisher]), we transfected siR-NAs into HCC cells.

Quantitative reverse-transcription polymerase chain reaction (qRT–PCR)

We extracted RNA using TRIzol reagent (Invitrogen) and then synthesized complementary deoxyribonucleic acid (cDNA) using SuperScript II reverse transcriptase (TaKaRa Bio, Dalian, China). Gene expression was analysed via qRT−PCR using a SYBR Green PCR kit.

Quan *et al. Journal of Translational Medicine*   (2025) 23:564

Page 3 of 18

Glyceraldehyde 3-phosphate dehydrogenase (GAPDH) served as the housekeeping gene, and gene transcription levels were quantified in terms of fold changes (FCs) using the $2^{-\Delta\Delta Ct}$ method. The primer sequences are presented in Supplementary Table 1.

Western blot

We extracted total protein from tissues and cells using radioimmunoprecipitation assay (RIPA) lysis buffer with 1% phenylmethylsulfonyl fluoride (PMSF; Solarbio Life Sciences, Beijing, China). We separated proteins via sodium dodecyl sulfate−polyacrylamide gel electrophoresis (SDS−PAGE) and transferred them to polyvinylidene difluoride (PVDF) membranes. The membranes were blocked with 5% skim milk and incubated with primary and secondary antibodies (Abs). Immunoreactive bands were visualized via an electrochemiluminescence (ECL) solution. The band intensity was quantified using ImageJ. The primary Abs used are listed in Supplementary Table 2.

Immunohistochemistry

Xenografted and human HCC tumour tissues were fixed in paraffin and sectioned. We incubated the sections with diluted primary Abs for 2 h and then with secondary Abs for another 2 h at 37 °C. Staining was performed using 3,3′-diaminobenzidine (DAB; Thermo Fisher) and haematoxylin. We mounted the slides with neutral gum and examined them under a NanoZoomer S60 (Hamamatsu, Japan). Positive cell percentages were classified into four categories: Category 1, 0−25%; Category 2, 26−50%; Category 3, 51−75%; and Category 4, 76−100%. The staining intensity was rated as 0 for negative, 1 for weak, 2 for moderate, or 3 for strong. Multiplying these scores resulted in the determination of the staining index. The Abs used are detailed in Supplementary Table 2.

Coimmunoprecipitation

Protein A/G magnetic beads (Thermo Fisher Scientific [Thermo Fisher]) were used for coimmunoprecipitation (Co-IP) assays. After the cells were isolated, the total proteins were incubated with diluted primary Abs (AP5Z1, TRIM21, PTEN, and haemagglutinin [HA]-tag) and NC immunoglobulin G (IgG) overnight at 4 °C. Then, prewashed A/G beads were added, and the mixture was incubated for 2 h at room temperature. Using SDS sample buffer at 95 °C, the proteins were eluted for Co-IP protein blotting.

Cell proliferation assay

For Cell Counting Kit-8 (CCK-8; Dojindo Molecular Technologies, Inc., Kumamoto, Japan) analysis, we incubated cells that had been transfected for 24 h in a 96-well plate (1000 cells/well). The samples were incubated at 37 °C with 10 μL of CCK-8 solution and 90 μL of culture medium per well for 2 h. We measured the absorbance at 450 nm using a microplate reader (Molecular Devices, Sunnyvale, CA, USA). The colony formation assay was conducted with 800 transfected cells per well on 6-well plates over 14 days. We fixed colonies with paraformaldehyde (PFA), stained them with crystal violet (Beyotime), and quantified them using ImageJ.

A Click EdU-594 Cell Proliferation Assay Kit (Beyotime) was used to label the transfected cells with 5-ethynyl-2′-deoxyuridine (EdU) for 4 h at 37 °C. We fixed the cells with formaldehyde, permeabilized them with Triton X-100, incubated them with the Click-iT mixture in the dark for 30 min to cause a reaction, stained them with 4′,6-diamidino-2-phenylindole (DAPI), and photographed them under an inverted fluorescence microscope (Olympus Corp., Tokyo, Japan).

Flow cytometric analysis of the cell cycle and apoptosis

We used flow cytometry (FCM) to analyse the cell cycle distribution of transfected cells from the abovementioned 6-well plates. The cells were fixed in 70% ethanol at 4 °C for 12 h, stained with propidium iodide (PI; LiankeBio, Hangzhou, China) and RNase at 37 °C for 30 min, and then subjected to FCM. To assess apoptosis, we treated cells with Annexin V (APC) and 7-AAD (LiankeBio). After gentle vortexing, the samples were incubated in the dark for 5 min at RT before analysis. All flow cytometry analyses were performed using FACSARia III (BD Pharmingen, San Diego, CA, USA).

Autophagy assay

Following the manufacturer's guidelines, we transiently transfected a green fluorescent protein (GFP)–mCherry–light chain 3 (LC3) vector (Guangzhou Aiji Bio-Technology Co., Ltd., Guangzhou, China) into cells using Lipofectamine 3000. Images were randomly taken 24 h posttransfection under an inverted fluorescence microscope (Olympus Corp., Tokyo, Japan).

Transmission electron microscopy

The transfected cells were subjected to trypsin digestion. They were fixed in 2.5% glutaraldehyde at 4 °C overnight and then in 1% osmium tetroxide (Ted Pella, Inc., Redding, CA, USA) at RT overnight. Next, we embedded them in Epon 812 resin and sectioned them to 60−80 nm using an ultramicrotome. Transmission electron microscopy (TEM; HT7800; Hitachi, Tokyo, Japan) was used to image the samples.

Mass spectrometry

After protein overexpression, we separated the proteins via SDS−PAGE and stained the gel with Fast Silver Stain Kits (Beyotime). Differential bands were trypsin-digested

in the gel; the peptides were dried, redissolved in Nano-LC mobile phase A, and analysed via liquid chromatography−mass spectrometry (LC–MS) using an EASY-nLC 1200 Nano Liquid Chromatography System and a Q Exactive mass spectrometer (both Thermo Fisher). IgG was used as the negative control.

Transcriptome sequencing

Following the manufacturer's guidelines, we extracted total RNA from cells with and without *AP5Z1* KD using an RNeasy Mini Kit (QIAGEN, Hilden, Germany). Expression Console software (Affymetrix, Santa Clara, CA, USA) was used to normalize the data with the robust multiarray average (RMA) algorithm. Custom Perl scripts were used to process raw reads for adapter removal and quality control. The *P* value cut-off for significant differential expression was 0.05, and gene upregulation and downregulation were ≥4-fold. We conducted an analysis of genes that were expressed at varying levels via Gene Ontology (GO; http://www.geneontology.org) and the Kyoto Encyclopedia of Genes and Genomes (KEGG; http://genome.jp/kegg), focusing on the differential expression patterns of these genes.

Animal models

We obtained 4-week-old nude BALB/c mice from the Experimental Animal Center of GMU. All the animal protocols adhered to the GMU guidelines for laboratory animal care and were approved by its Ethics Review Committee. We subcutaneously inoculated a total of 2×10^6 cells into the left axillary region of the mice ($n = 5$). During the experiment, tumour diameters were measured weekly for 4 weeks, and tumour tissues were excised, measured, and photographed after mouse euthanasia. Finally, we fixed part of the tumour and embedded it in paraffin for subsequent tests.

Bioinformatics analysis

We obtained STAR count data and clinical information for HCC tumours from the TCGA database (The Cancer Genome Atlas; National Cancer Institute [NCI], Bethesda, MD, USA). We then extracted the data in TPM format and performed normalization using the $\log2(\text{TPM} + 1)$ transformation. R software (version 4.0.3) was used for data analysis. A p value of less than 0.05 was considered statistically significant.

Data analysis

We analysed the data using GraphPad Prism version 8.0 (GraphPad Software, Inc., San Diego, CA, USA). *AP5Z1* expression and clinical parameters were assessed using the Wilcoxon rank-sum test, whereas Kaplan−Meier analysis was used to compare overall survival (OS) between groups. The experiments were performed in triplicate, and the results are presented as the means ± standard deviations (SDs). We determined statistical significance using Student's *t* test or one-way analysis of variance (ANOVA).

Results

AP5Z1 expression was upregulated in HCC tissues and associated with a poor prognosis

As previously mentioned, members of the AP family play significant roles in tumour development and tumorigenesis. Mutations in the AP5Z1 gene can lead to neurological disorders; nevertheless, it remains unclear whether AP5Z1 plays a role in the development and progression of HCC. Hence, we carried out further analysis to determine the role of AP5Z1 in HCC. We collected 60 pairs of samples from primary HCC patients and adjacent normal tissues and used qRT−PCR to verify *AP5Z1* expression in the tumour tissues. These tissues presented significantly higher levels of *AP5Z1* than adjacent normal tissues did (Fig. 1A). Kaplan−Meier analysis revealed shorter OS in HCC patients with higher *AP5Z1* expression (Fig. 1B).

Subsequent Western blot (WB) analysis demonstrated significantly increased *AP5Z1* protein levels in tumour tissues from primary HCC patients compared with adjacent normal tissues (Fig. 1C). Immunohistochemical (IHC) analysis revealed robust staining for *AP5Z1* in tumour tissues, in contrast to the weak positive staining observed in adjacent normal tissues (Fig. 1D). The expression levels of *AP5Z1* were subsequently examined in five HCC cell lines (MHCC-97 H, HUH-7, SUN-182, SUN-449, and LM3) as well as in human normal liver cells (MIHA). We observed a significant difference between cancer cell lines and normal liver cells (Fig. 1E and F). Among the HCC cell lines examined, SUN-449 and LM3 presented the most substantial increases in *AP5Z1* expression, whereas MHCC-97 H cells presented a relatively modest increase. Therefore, we conducted KD experiments on the SUN-449 and LM3 cell lines and OE experiments on the MHCC-97 H cell line. The results confirmed the successful generation of cell lines with stable *AP5Z1* KD or OE (Supplementary Fig. 1A, 1B). Furthermore, protein expression levels also confirmed the successful construction of KD and OE lines (Supplementary Fig. 1C).

Our analysis of the TCGA database revealed that AP5Z1 was strongly overexpressed in primary HCC. Furthermore, patients with elevated levels of *AP5Z1* expression tended to present with increased tumour–node–metastasis (TNM) stages (Fig. 1G-J). According to the Kaplan−Meier survival analysis of the TCGA dataset, these patients had significantly lower OS and disease-free survival (DFS) rates. These results indicated that *AP5Z1* was correlated with a poor prognosis in HCC patients (Fig. 1K and L). We subsequently investigated the clinical
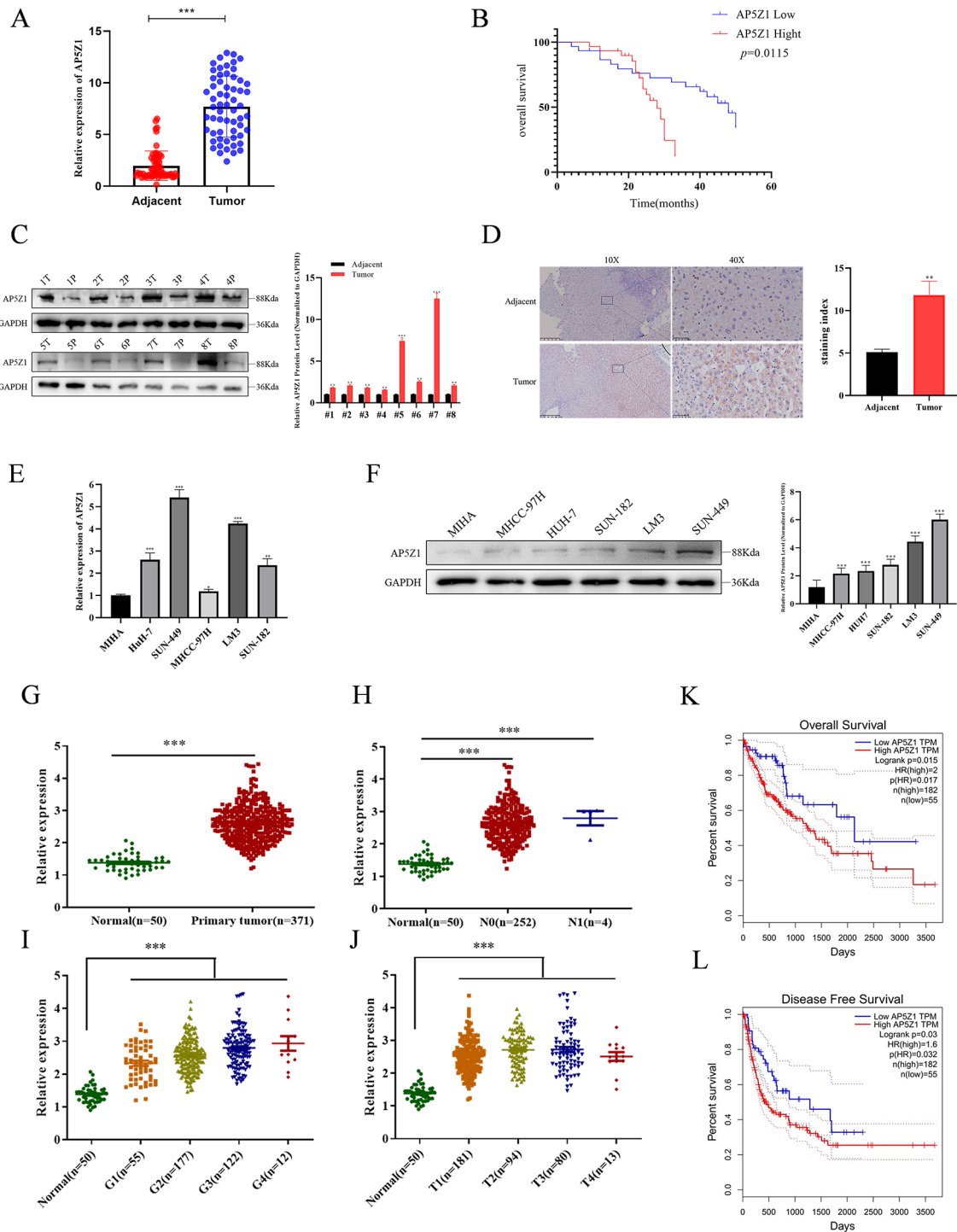
Fig. 1 Upregulation of *AP5Z1* expression in HCC and its association with a poor prognosis. (**A**) Quantitative RT–PCR validation of *AP5Z1* expression in 60 pairs of cancer tissues and adjacent normal tissues. (**B**) Kaplan–Meier survival analysis showing the OS rates of 60 HCC patients stratified by the *AP5Z1* expression level. (**C**) Western blot analysis of AP5Z1 expression in eight pairs of hepatocellular carcinoma tissues and adjacent normal tissues. (**D**) Representative images of *AP5Z1* expression in tumour tissues and adjacent normal tissues as determined by IHC staining. Scale bar = 250 μm (Left). Scale bar = 50 μm (right). (**E**) Analysis of AP5Z1 expression in normal liver cells (MIHAs) and five cancer cell lines (Huh7, SUN-449, MHCC97H, LM3, and SUN-182) via RT–PCR. (**F**) Analysis of AP5Z1 expression in normal liver cells (MIHAs) and five cancer cell lines (Huh7, SUN-449, MHCC97H, LM3, and SUN-182) using Western blotting. (**G-J**) TCGA analysis: AP5Z1 is upregulated in tumors (*n* = 371) vs. normal (*n* = 50) (**G**), higher in metastatic (N1, *n* = 4) vs. non-metastatic (N0, *n* = 252) tumors (**H**), and increases with histological grade (G1-G4, *n* = 55/177/122/12) (**I**) and TNM stage (T1-T4, *n* = 181/94/80/13) (**J**). (**K-L**) High AP5Z1 correlates with reduced OS and DFS. The results are shown as the mean ± standard error (SE) of three separate experiments. Significance levels are denoted by * for *P* < 0.05, ** for *P* < 0.01, and *** for *P* < 0.001

prognostic significance of AP5Z1 in our cohort of HCC patients. The cohort (mean age: 54.6 ± 12.8 years; median age: 58 years, IQR: 45–67) exhibited a left-skewed age distribution (median > mean), suggesting that the median better reflects the central tendency in this population with more older participants. Our results revealed that AP5Z1 expression was significantly associated with tumour size, lymph node invasion, and distant metastasis in HCC patients (Table 1). High AP5Z1 expression was correlated with a poor prognosis.

AP5Z1 regulated HCC cell proliferation and apoptosis

To elucidate the role of *AP5Z1* in HCC (HCC) cell proliferation, we collected transfected cells and conducted a series of experiments. The CCK-8 results demonstrated that, in comparison with that in the control group, cell viability was diminished in *AP5Z1* KD SUN-449 and LM3 cells, whereas it was increased in *AP5Z1* OE MHCC-97 H cells, with statistically significant differences observed on day 4. As shown by colony formation assays, AP5Z1 OE increased the clonogenic potential of HCC cells in vitro,

whereas *AP5Z1* KD impaired it (Fig. 2A and B). Furthermore, the results of the EdU staining assay demonstrated that elevated expression of *AP5Z1* enhanced cellular DNA synthesis, whereas suppression of AP5Z1 inhibited DNA synthesis in HCC cells (Fig. 2C).

Given the critical role of the cell cycle in cell proliferation [17, 18], we used FCM to study the effect of *AP5Z1* on cell cycle progression. A significant increase in G0/G1 phase cells was observed in the *AP5Z1* KD groups compared with the control groups, with an accompanying decrease in S phase cells. The *AP5Z1* OE groups presented the opposite trend (Fig. 2D).

We then used FCM to assess the effect of *AP5Z1* on cellular apoptosis. Our results revealed that the KD of *AP5Z1* increased apoptosis, whereas OE inhibited it (Fig. 2F). Next, the cell cycle and apoptosis protein levels in transfected HCC cells were examined via WB. According to these findings, the expression of cell cycle-related proteins (CDK2, CDK4, cyclin D1, and cyclin E1) was significantly decreased following AP5Z1 KD, whereas their expression was increased after *AP5Z1* OE (Fig. 2E).

Table 1 Clinical-pathological correlations between AP5Z1 and HCC in a cohort of 60 patients

Variables	Number of Participants (*n* = 60)	Low AP5Z1 experssion (*n* = 30)	High AP5Z1 experssion (*n* = 30)	*P*
Age(years)	60			
< 50	25	12	13	0.7940
≥ 50	35	18	17	-
Mean Age (Mean ± SD)	54.6 ± 12.8	53.2 ± 13.1	56.0 ± 12.5	0.4120
Median Age (Median [IQR])	58 [45–67]	56 [44–65]	60 [46–68]	0.3890
Gender	60			
Male	29	15	14	0.7961
Female	31	15	16	-
HBV infection	60			
Positive	24	14	10	0.2918
Negative	36	16	20	-
Tumor size (cm)	60			
< 5	20	16	4	0.0010
≥ 5	40	14	26	-
TNM stage	60			
I-II	23	17	6	0.0035
III–IV	37	13	24	-
Lymph node invasion	60			
Absent	27	19	8	0.0043
Present	33	11	22	-
Metastasis	60			
No	28	18	10	0.0384
Yes	32	12	20	-

Notes:

1.The Mean Age represents the arithmetic mean of all patients' ages, while the Median Age is the value located in the middle when all ages are sorted from smallest to largest. A higher median age than the mean age indicates a left-skewed (negatively skewed) age distribution, suggesting that the median may more accurately reflect the central age characteristic of the patients compared to the mean

2.SD denotes Standard Deviation, and IQR denotes Interquartile Range

3.P-values are used to compare differences between the low and high expression groups. A P-value < 0.05 indicates a statistically significant difference

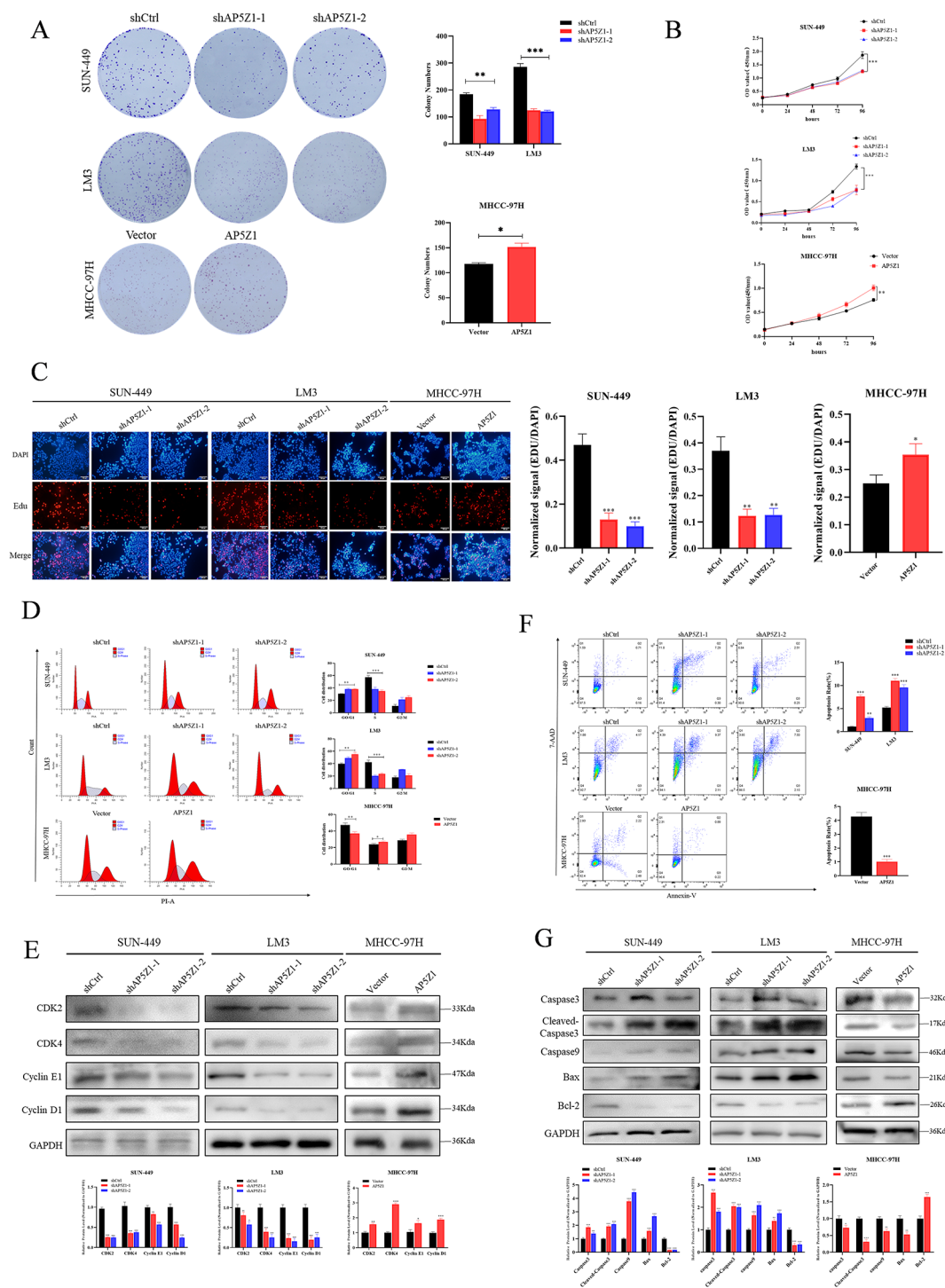4.Total participants: 60 HCC patients

Fig. 2 Influence of *AP5Z1* on the in vitro proliferation of HCC cells. (**A**) Assessment of the impact of AP5Z1 on HCC cell proliferation through colony formation tests. (**B**) CCK-8 assay to determine the influence of AP5Z1 on the proliferation of HCC cells. (**C**) The EdU incorporation test was used to assess the effect of AP5Z1 on DNA synthesis in hepatocellular carcinoma cells. Scale bar = 100 μm. (**D**) FCM analysis of the regulatory effect of AP5Z1 on the HCC cell cycle. (**F**) FCM was used to assess the effect of *AP5Z1* on the apoptosis of HCC cells. In addition, WB analysis was conducted to evaluate the influence of *AP5Z1* expression on proteins associated with the cell cycle and apoptosis in HCC cells (**E, G**). The results are shown as the mean ± standard error (SE) of three separate experiments. Significance levels are denoted by * for *P* < 0.05, ** for *P* < 0.01, and *** for *P* < 0.001
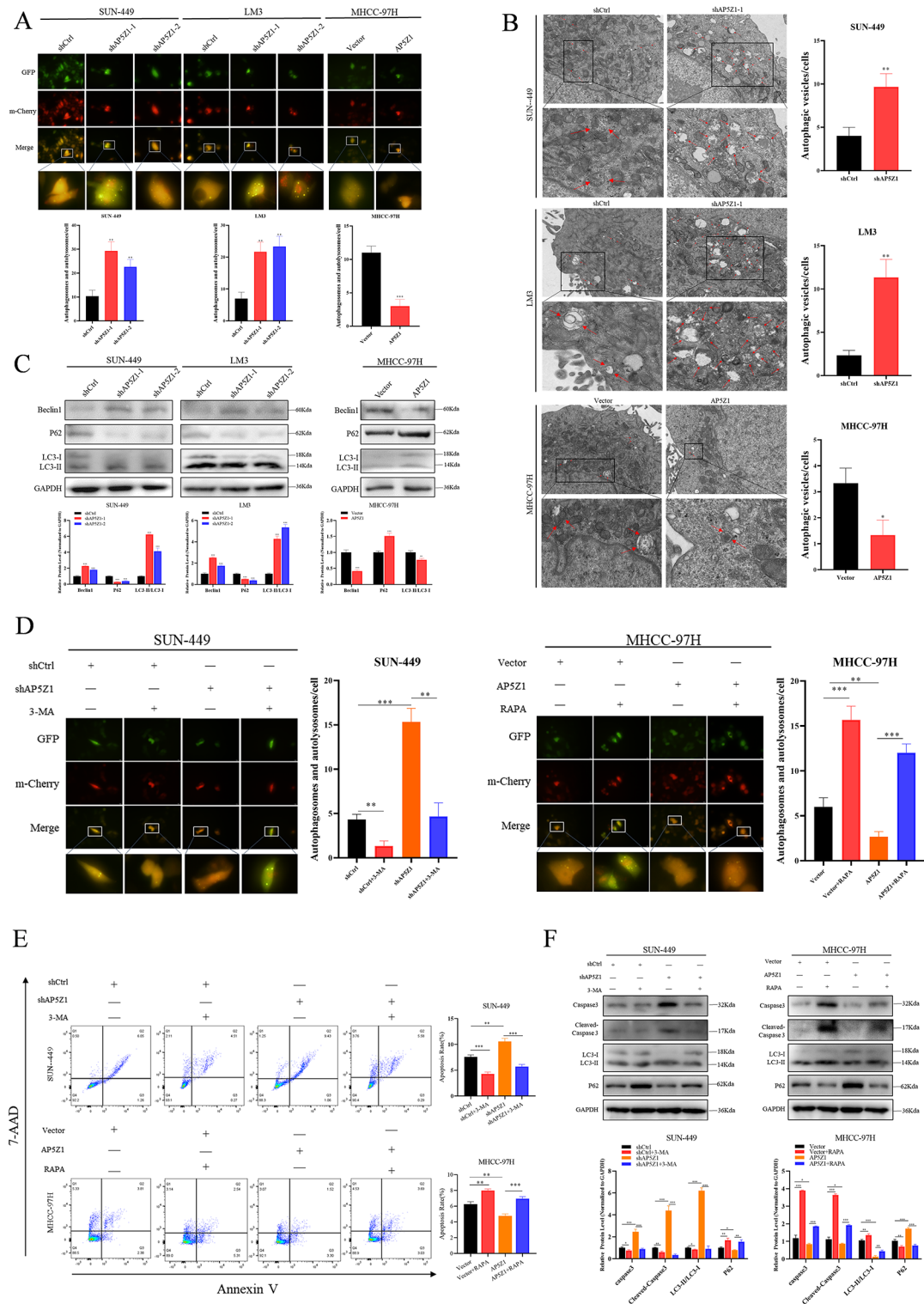
Fig. 3 (See legend on next page.)

As a pivotal cell cycle protein, cyclin D1 facilitates progression from G1 to S phase by interacting with CDK4 [19]. Similarly, cyclin E serves as a crucial regulatory subunit of CDK2, forming the cyclin E/CDK2 complex,

which predominantly operates during the late G1 phase of the cell cycle [20, 21]. Throughout the process of apoptosis, the cysteine–aspartic acid–specific protease/proteinase (caspase) family plays a crucial role. Specifically,

(See figure on previous page.)

Fig. 3 *AP5Z1* inhibited autophagy in HCC cells and modulated apoptosis through autophagic pathways. (**A**) The distribution of GFP–mCherry–LC3B in transfected cells was observed under an inverted fluorescence microscope. Scale bar = 20 µm. (**B**) TEM was used to observe the effect of AP5Z1 on autophagy in cells. The arrows indicate autophagosomes or autolysosomes. Scale bar = 2 µm. (**C**) WB analysis was conducted to assess the effects of *AP5Z1* expression on the levels of autophagy-related proteins in HCC cells. (**D**) After the KD or OE of *AP5Z1*, the cells were treated with 3-MA(5mM,12 h treatment) or RAPA(10ng/ml,12 h treatment), and the distribution of GFP–mCherry–LC3B was examined under an inverted fluorescence microscope. Scale bar = 20 µm. (**E, F**) After the KD or OE of *AP5Z1*, cells were treated with 3-MA(5mM,12 h treatment)/RAPA(10ng/ml,12 h treatment). The apoptosis rate was subsequently assessed using Annexin V/PI double staining (**E**), while WB analysis was used to detect proteins associated with apoptosis and autophagy (**F**). The results are shown as the mean ± standard error (SE) of three separate experiments. Significance levels are denoted by * for $P < 0.05$, ** for $P < 0.01$, and *** for $P < 0.001$

Caspase-9 functions as an apoptotic initiator, whereas Caspase-3 serves as an apoptotic effector. The mature form of Caspase-3, known as cleaved Caspase-3, is generated following its cleavage and activation [22].

By evaluating apoptosis-related protein expression via WB analysis, we observed that AP5Z1 KD markedly activated Bcl-2-like protein 4 (Bax), Caspase-9, Caspase-3, and cleaved Caspase-3, whereas Bcl-2-like protein 2 (Bcl-2) expression was decreased. Conversely, *AP5Z1* OE in MHCC-97 H cells resulted in an increase in Bcl-2 expression and a significant inhibition of caspase activation (Fig. 2G). As demonstrated by in vitro gain- and loss-of-function experiments, *AP5Z1* regulated the cell cycle of HCC cells. Furthermore, as an oncogene, *AP5Z1* facilitates HCC cell proliferation while concurrently inhibiting apoptosis.

AP5Z1 modulated autophagy levels in hepatocellular carcinoma cells and regulated cellular apoptosis via autophagy

Previous research has demonstrated that *AP5Z1* is integral to the regulation of lysosomal and autophagic processes [9, 23]. However, the precise regulatory mechanisms involved require further elucidation, and the potential role of *AP5Z1* in cancer has not been documented to date. To analyse whether AP5Z1 affects autophagy levels in tumour cells, we employed a GFP–mCherry–LC3B dual-fluorescence system. Our results demonstrated that, compared with control cells, *AP5Z1* KD HCC cells presented increased numbers of yellow puncta (autophagosomes) and red puncta (autolysosomes). Conversely, decreases in these puncta were observed in the *AP5Z1* OE cell lines (Fig. 3A).

Next, we harvested the transfected cells and examined the numbers of autophagosomes and autolysosomes within these cells using TEM. The results revealed a significant increase in the number of autophagosomes in cells subjected to *AP5Z1* KD, whereas those with *AP5Z1* OE presented comparatively lower numbers of autophagosomes (Fig. 3B). Consistent results were obtained through immunoblotting for autophagy-related proteins. Specifically, *AP5Z1* KD resulted in the upregulation of light chain 3 II and I (LC3II, LC3I) and Beclin 1 levels and the downregulation of sequestosome-1 (SQSTM1)/p62

levels. AP5Z1 regulated autophagy in HCC cells according to these findings (Fig. 3C).

We employed the autophagy inhibitor 3-methyladenine (3-MA) and the autophagy inducer rapamycin (RAPA) to investigate the link between AP5Z1 and autophagy in HCC cells. These findings revealed that 3-MA treatment effectively reversed the activation of autophagy induced by AP5Z1 KD. Conversely, RAPA treatment counteracted the suppression of autophagy resulting from *AP5Z1* OE (Fig. 3D). In addition, Annexin V–APC and 7-AAD double staining revealed that the inhibition of autophagy via 3-MA reduced the degree of apoptosis induced by *AP5Z1* KD in SUN-449 cells. Conversely, the activation of autophagy via RAPA reversed the suppression of apoptosis associated with *AP5Z1* OE (Fig. 3E). WB analysis revealed that *AP5Z1* KD SUN-449 cells treated with 3-MA presented downregulation of apoptosis-related proteins. Conversely, the reduced expression of apoptosis-related proteins induced by *AP5Z1* OE was reversed by treatment with RAPA, an autophagy agonist (Fig. 3F). These findings suggest that *AP5Z1* modulates cell apoptosis by regulating autophagy.

AP5Z1 interacted with PTEN to modulate the PI3K/Akt/mTOR signalling pathway

To identify the main target genes regulated by AP5Z1 in cell apoptosis and autophagy, we conducted RNA-seq on AP5Z1-knockdown cells to identify the signalling pathways involved in AP5Z1-mediated apoptosis and autophagy. According to our results, PI3K/Akt signalling is critical for the regulation of these processes (Fig. 4A). Thirty-nine genes exhibited differential expression in the PI3K/Akt pathway (Supplementary Fig. 2A). Furthermore, analysis of the TCGA database revealed a link between *AP5Z1* expression and the PI3K/Akt pathway (Supplementary Fig. 2B). Within the PI3K/Akt signalling cascade, mTOR serves as a principal downstream effector. Research has shown that mTOR complex 1 (mTORC1) is an important regulator of autophagy, acting at several stages, including nucleation, elongation, maturation, and termination [24]. We further validated the regulatory role of AP5Z1 in the PI3K/Akt/mTORC signaling pathway. The experimental results showed that knockdown of AP5Z1 decreased the phosphorylation levels of key factors in this pathway, while the total
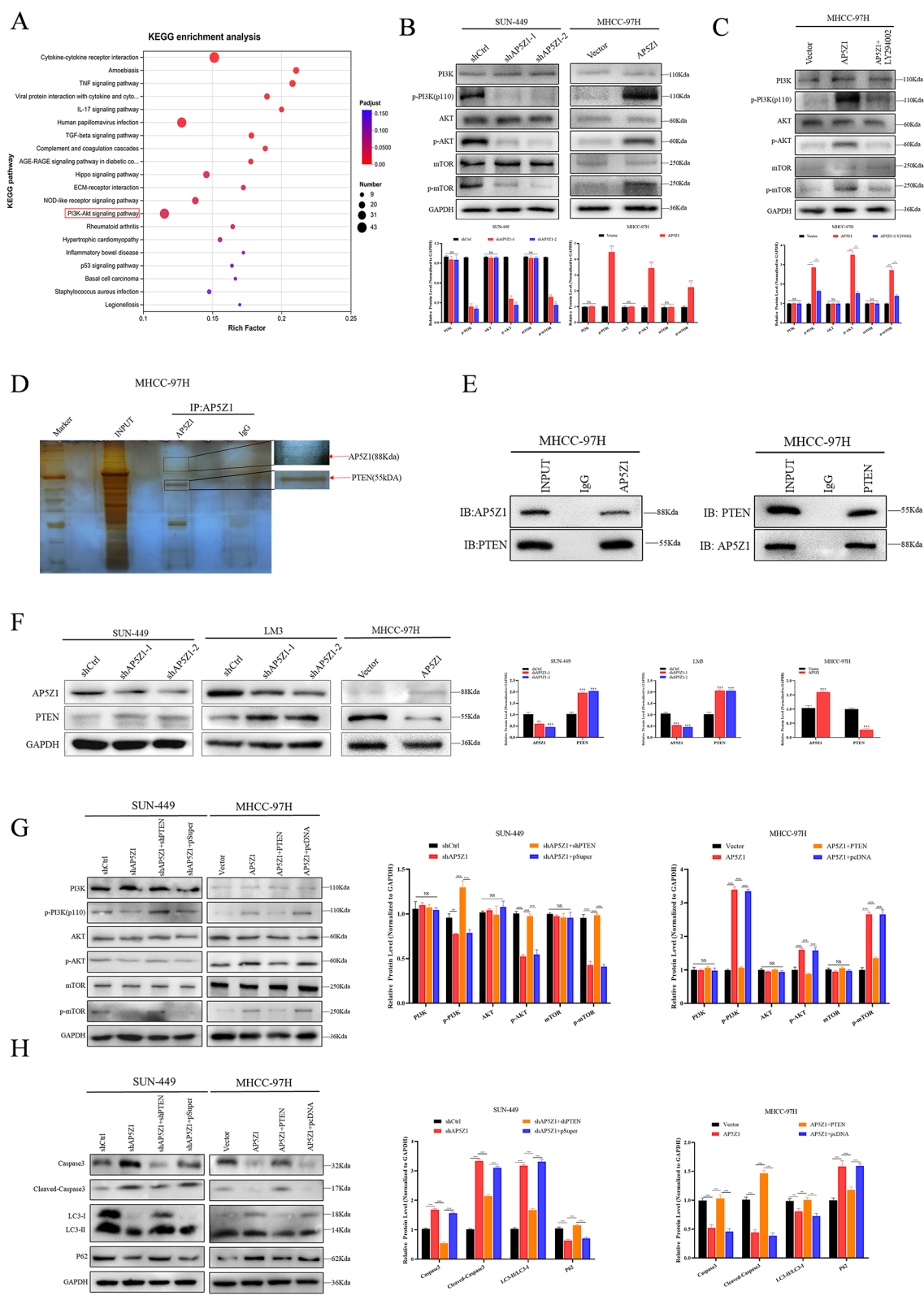
Fig. 4 (See legend on next page.)

(See figure on previous page.)

Fig. 4 *AP5Z1* modulates cellular apoptosis and autophagy via the PTEN/PI3K/Akt/mTOR signalling cascade. (**A**) KEGG pathway enrichment analysis of genes regulated by *AP5Z1*, as visualized in a bubble chart. (**B**) WB analysis was performed to examine the effects of AP5Z1 knockdown and overexpression on the PI3K/Akt/mTOR signaling pathway. (**C**) WB analysis was performed to examine the effects of LY294002 (25 μM,24 h treatment) on the PI3K/Akt/mTOR signaling pathway in AP5Z1-overexpressing cellular models. (**D**) Identification of AP5Z1-binding proteins isolated from MHCC-97 H cell lysates through silver staining. The red arrow denotes the specific binding band of *AP5Z1* and PTEN. IgG served as a negative control. (**E**) Verification of the presence of *AP5Z1* and PTEN in the coprecipitated complex was conducted via Co-IP. (**F**) WB analysis analysis showing the effect of *AP5Z1* OE or KD on PTEN levels. (**G**) WB analysis of the effects of *AP5Z1* KD or OE and subsequent PTEN rescue on total and phosphorylated proteins within the PI3K/Akt/mTOR signalling pathway. (**H**) WB analysis evaluating the influence of *AP5Z1*-mediated PTEN rescue on proteins associated with apoptosis and autophagy. The results are shown as the mean ± standard error (SE) of three separate experiments. Significance levels are denoted by * for $P < 0.05$, ** for $P < 0.01$, and *** for $P < 0.001$. NS for $P > 0.05$

protein levels remained unchanged. Conversely, overexpression of AP5Z1 increased the phosphorylation levels of these factors (Fig. 4B, Supplementary Fig. 2C). To further confirm this, we performed rescue experiments. The results demonstrated that the PI3K/Akt/mTORC signaling pathway inhibitor LY294002 could reverse the increase in phosphorylation levels caused by AP5Z1 overexpression (Fig. 4C). These findings indicate that AP5Z1 exerts its biological functions by modulating the PI3K/Akt/mTORC signaling pathway.

To further understand the molecular mechanisms by which AP5Z1 may function in HCC cells, we conducted Co-IP experiments to identify proteins that interact with *AP5Z1*. As shown in Fig. 4D, the silver-stained SDS−PAGE gel revealed distinct differential bands for *AP5Z1* compared with the IgG control. Differential bands were subsequently separated and subjected to trypsin digestion for MS analysis. Among the identified candidate proteins, we selected PTEN for further investigation because of its significant role as a tumour suppressor and its close association with the PI3K/Akt signalling pathway. Subsequent Co-IP assays validated the interaction between AP5Z1 and PTEN (Fig. 4E). Furthermore, the expression levels of AP5Z1 were inversely associated with those of PTEN (Fig. 4F).

To determine whether *AP5Z1* modulates the PI3K/Akt/mTORC pathway via PTEN, we conducted a series of rescue experiments. In AP5Z1-knockdown cells, PTEN co-knockdown significantly reversed the decreased phosphorylation levels of p-PI3K, p-Akt, and p-mTOR, which were induced by AP5Z1 knockdown. Conversely, in AP5Z1-overexpressing cells, re-expression of PTEN effectively antagonized the activation of p-PI3K, p-Akt, and p-mTOR phosphorylation by AP5Z1 (Fig. 4G). Further examination of apoptosis and autophagy markers revealed that PTEN co-knockdown reversed the enhancement of autophagy and increase in apoptosis caused by AP5Z1 knockdown, whereas PTEN overexpression reversed the inhibition of autophagy and reduction in apoptosis caused by AP5Z1 overexpression (Fig. 4F). These results indicate that AP5Z1 regulates the PI3K/Akt/mTOR pathway activity via PTEN, thereby modulating autophagy and apoptosis.

AP5Z1 influenced ubiquitination and degradation of the PTEN protein via the recruitment of TRIM21

In this study, we identified an interaction between AP5Z1 and the PTEN protein, with the levels of AP5Z1 inversely correlated with those of the PTEN protein. We then performed RT−qPCR analysis and found that neither knockdown nor overexpression of AP5Z1 altered PTEN mRNA levels, indicating that AP5Z1 primarily regulates PTEN through posttranslational modifications (Fig. 5A). We subsequently explored whether AP5Z1 regulates PTEN degradation via the ubiquitin–proteasome pathway. Treatment with the proteasome inhibitor MG132 significantly diminished the differences in PTEN protein levels in HCC cells (Fig. 5B), suggesting that AP5Z1 may regulate PTEN through the ubiquitin−proteasome system. In further experiments, we used cycloheximide (CHX) to inhibit protein synthesis and analysed the effect of AP5Z1 on the half-life of the PTEN protein. AP5Z1 knockdown significantly prolonged the half-life of the PTEN protein in HCC cells, whereas AP5Z1 overexpression significantly shortened it (Fig. 5C). Additionally, ubiquitination assays revealed that AP5Z1 knockdown markedly reduced PTEN ubiquitination levels, whereas AP5Z1 overexpression significantly increased PTEN ubiquitination (Fig. 5D). Collectively, these findings demonstrate that AP5Z1 mediates PTEN protein degradation through ubiquitination.

To identify the key E3 ubiquitin ligase responsible for AP5Z1-mediated PTEN ubiquitination, we performed mass spectrometry analysis to identify proteins that interact with AP5Z1 and found that TRIM21 may be a critical factor. TRIM21, known for its E3 ubiquitin ligase activity, facilitates the ubiquitination of substrate proteins [25]. Coimmunoprecipitation (Co-IP) experiments confirmed the interaction among AP5Z1, PTEN, and TRIM21 (Fig. 5E). Additionally, the expression level of TRIM21 was negatively correlated with the protein level of PTEN (Fig. 5F). On the basis of these results, we hypothesize that PTEN is a substrate of TRIM21 and that AP5Z1 recruits TRIM21 to promote its binding to PTEN, subsequently inducing the degradation of PTEN.

To verify the role of TRIM21 in PTEN ubiquitination, we conducted ubiquitination experiments. The results revealed that the knockdown of AP5Z1 and TRIM21
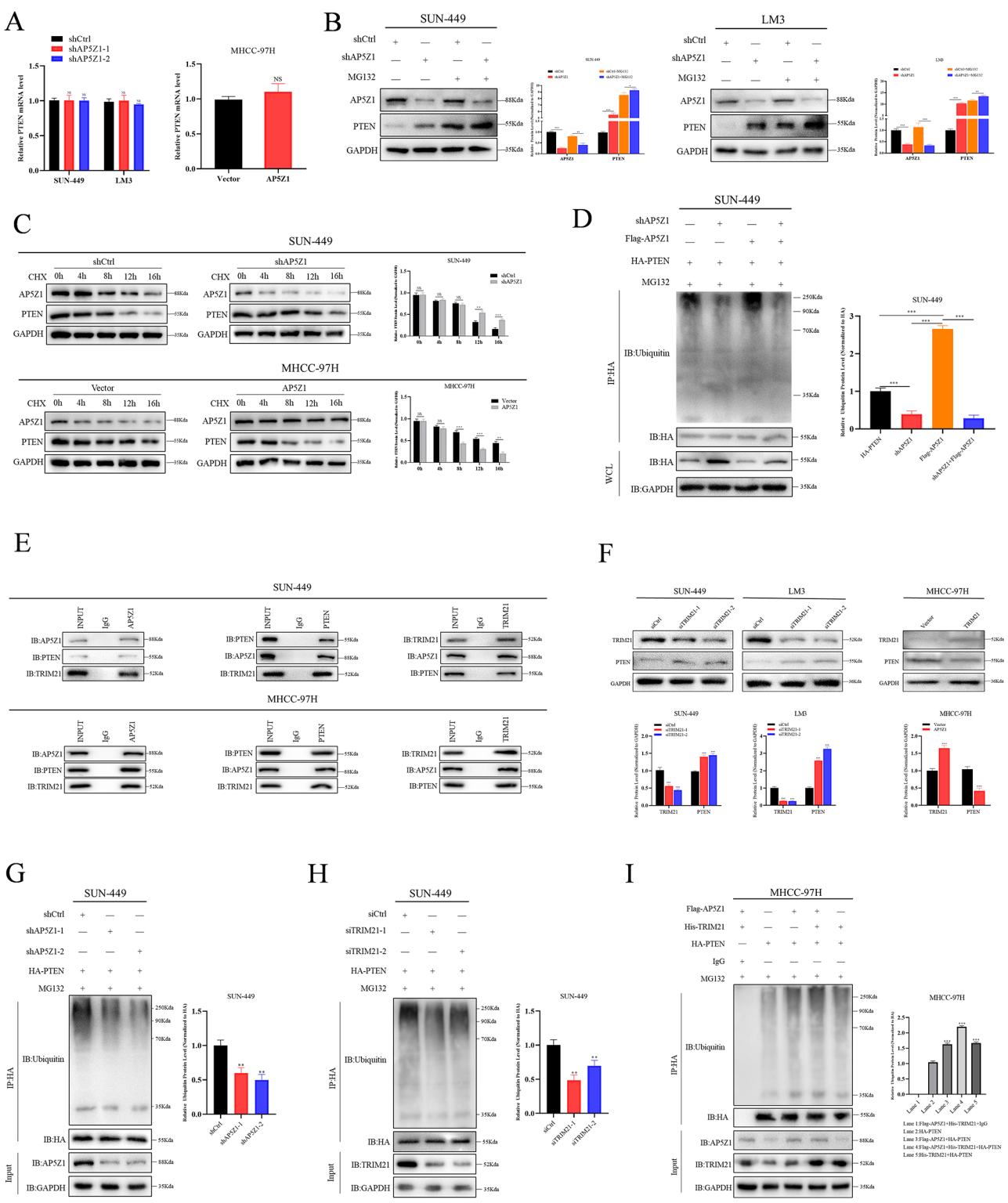
Fig. 5 (See legend on next page.)

significantly reduced PTEN ubiquitination levels in HCC cells, whereas the co-overexpression of AP5Z1 and TRIM21 significantly increased PTEN ubiquitination (Fig. 5G-I). These findings demonstrate that AP5Z1

promotes TRIM21-mediated PTEN ubiquitination, thereby regulating PTEN protein degradation.

(See figure on previous page.)

Fig. 5 AP5Z1 facilitated PTEN protein degradation via TRIM21-mediated ubiquitination. (**A**) RT–qPCR analysis of PTEN mRNA expression levels in AP5Z1-knockdown or AP5Z1-overexpressing HCC cells. (**B**) WB analysis of PTEN levels in AP5Z1 knockdown and control SUN-449 and LM3 cells stimulated with MG132 (10 µM) for 6 h. (**C**) The half-life of the PTEN protein was determined in AP5Z1-knockdown, AP5Z1-overexpressing, and control HCC cells using a 10 µM cycloheximide (CHX)-chase assay. (**D**) Ubiquitination levels of PTEN in AP5Z1-knockdown or AP5Z1-overexpressing SUN449 cells transfected with the corresponding plasmids (48 h) and treated with MG132 (10 µM, 6 h treatment). (**E**) Co-IP experiments demonstrated the endogenous interaction among AP5Z1, TRIM21, and PTEN. (**F**) Western blot analysis was performed to determine the effects of TRIM21 knockdown or overexpression on PTEN expression levels. (**G**) Ubiquitination levels of PTEN in AP5Z1-knockdown SUN-449 cells treated with MG132 (10 µM, 6 h treatment). (**H**) Ubiquitination levels of PTEN in TRIM21-knockdown SUN-449 cells treated with MG132 (10 µM, 6 h treatment). (**I**) Ubiquitination levels of PTEN in AP5Z1- and TRIM21-overexpressing MHCC-97 H cells treated with MG132 (10 µM, 6 h treatment). The results are shown as the mean ± standard error (SE) of three separate experiments. Significance levels are denoted by * for $P < 0.05$, ** for $P < 0.01$, and *** for $P < 0.001$. NS for $P > 0.05$

AP5Z1 inhibited tumorigenesis in a nude mouse model

We used nude mice to evaluate the effects of *AP5Z1* on tumorigenesis and development in vivo. The findings indicated that, relative to those in the control group, the growth rate of the subcutaneously transplanted tumours was significantly reduced, with concomitant decreases in tumours weight and volume following AP5Z1 knockdown. Next, we conducted in vivo rescue experiments to validate the growth of subcutaneously transplanted HCC tumours via the *AP5Z1*/PTEN axis. The results demonstrated that co-knockdown of PTEN could reverse the tumours suppression caused by AP5Z1 knockdown (Fig. 6A–C). We then used IHC to assess the expression of the tumours proliferation marker Ki-67 in the transplanted tumours. Consistent with the in vivo experimental results, we found that co-knockdown of PTEN reversed the AP5Z1 knockdown-induced decrease in proliferation levels of the xenografts (Fig. 6D). Taken together, these findings suggest that *AP5Z1* regulates PTEN expression to influence tumour growth and development in nude mice.

Discussion

Protein sorting and transport within cells are facilitated by heterotetrameric adaptor protein complexes. According to studies conducted in the 1980s, clathrin-coated vesicles (CCVs) are the main location of AP-1 and AP-2 [26, 27]. AP-3 and AP-4 were discovered in the 1990s and are both located in the trans-Golgi network (TGN) [28]. The fifth adaptor complex, AP-5, was identified in 2011 and is localized to late endosomes. Notably, its subunits exhibit very low sequence similarity with those of other adaptor complexes [29], suggesting that while members of the AP family share certain characteristics, they also show significant differences. In addition, AP-1 lacking the γ1-adaptin subunit has been demonstrated to prevent BC progression, whereas *AP3S1* KD affects OC cell migration and invasion [10, 12]. In this study, we found that *AP5Z1* KD inhibited the proliferation and promoted the apoptosis of HCC cells. These findings indicate that AP-5 regulates tumour progression in a manner similar to its other family members.

AP5Z1 colocalizes with lysosomal-associated membrane protein 1 (LAMP1), a marker for late endosomes and lysosomes, suggesting the presence of AP-5 within late endosomes. In addition, AP-5 A forms a complex with spastic paraplegia 11 and 15 (SPG11, SPG15), and its expression level seems to be inversely related to that of mTORC1 [30]. Mutations in *AP5Z1* or siRNA-mediated KD of *AP5Z1* closely mimic the phenotypic characteristics of lysosomal-storage diseases, indicating that AP-5 is critical to the homeostasis of endosomes and lysosomes [23]. The autophagy–lysosome degradation pathway is crucial for maintaining homeostasis at the cellular, tissue, and organismal levels. Through the process of autophagy, superfluous or dysfunctional cellular components are eliminated, and metabolic substrates are recycled, thereby sustaining cellular homeostasis and facilitating the renewal of cellular constituents [31, 32]. Autophagy is presently understood to play dual roles in cancer pathogenesis. In the initial stages of tumorigenesis, it might serve as a tumour suppressor. However, accumulating evidence suggests that in advanced cancers, autophagy helps tumour cells manage intracellular and environmental stressors, including hypoxia, nutrient deprivation, and cancer therapies, thereby promoting tumour progression [33–35]. Furthermore, AP-2 has been shown to exert a regulatory influence on the mechanism of cellular autophagy [36]. In this study, we observed that the KD of *AP5Z1* resulted in greater numbers of yellow puncta (autophagosomes) and red puncta (autolysosomes) in HCC cells, whereas *AP5Z1* OE had the opposite effect. The administration of 3-MA reversed the activation of autophagy induced by *AP5Z1* KD, whereas RAPA counteracted this inhibitory effect. While our findings demonstrate the regulatory role of AP5Z1 in autophagy, the precise molecular mechanisms underlying its control of lysosomal homeostasis remain to be fully elucidated.

Cell apoptosis, akin to autophagy, is a quintessential form of programmed cell death that is meticulously regulated by an array of genes. The elimination of superfluous or aberrant cells via apoptosis is essential in multicellular organisms [37–39]. Recent research has shown that apoptosis and autophagy can regulate one another, with autophagy potentially modulating cell death through the induction of apoptosis [40]. During this process, autophagy can synergize with apoptotic pathways to facilitate cell death [41]. Current evidence also suggests that
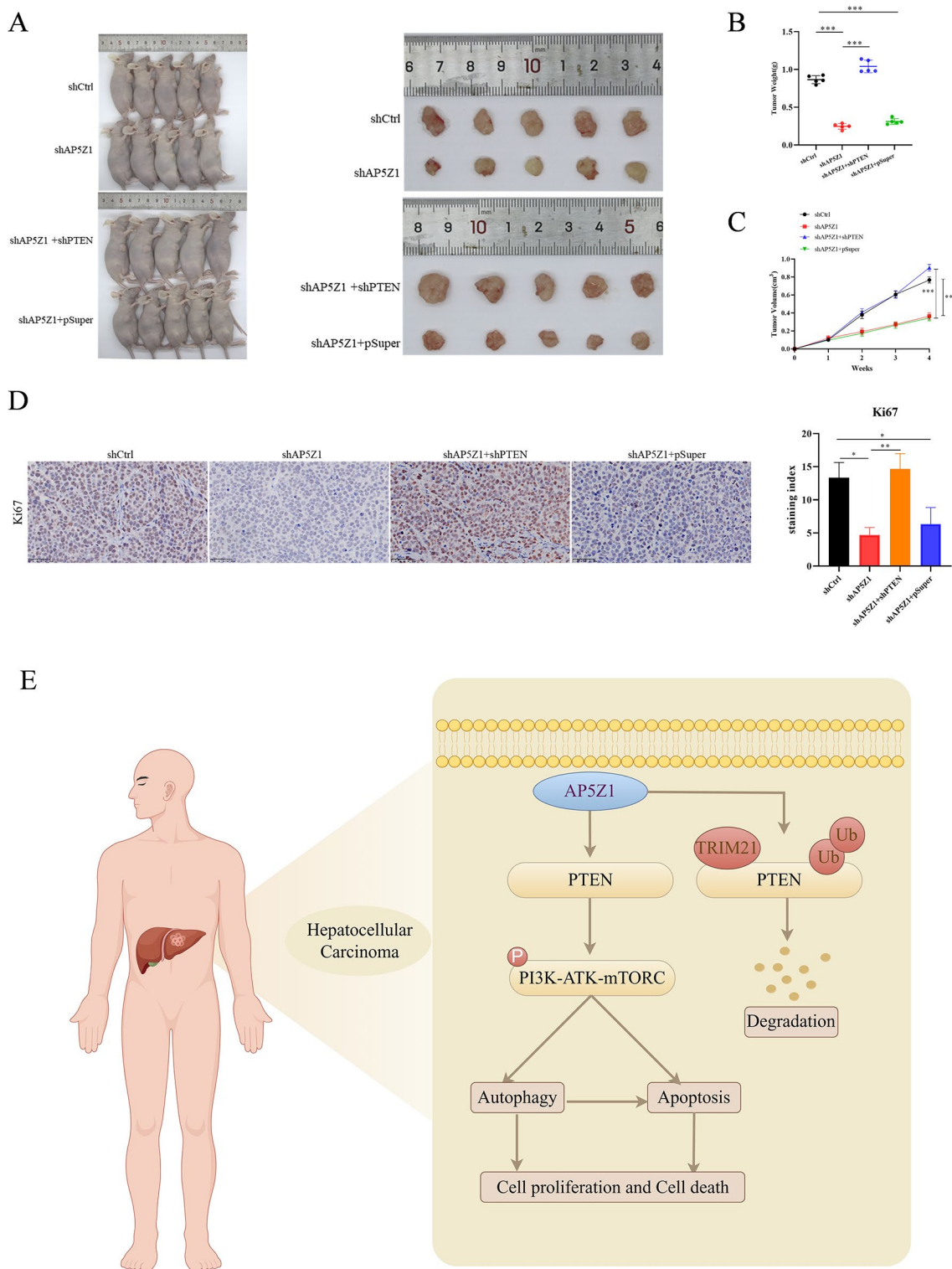
Fig. 6 *AP5Z1* facilitates HCC tumorigenesis via the modulation of PTEN. (**A–C**) Tumour formation assays in nude mice were conducted to validate the effect of the *AP5Z1*–PTEN interaction on HCC tumorigenesis (*n* = 5) (**A**). Measurements of tumour weight (**B**) and tumour growth rate (**C**) were recorded. (**D**) IHC analysis was performed to assess the expression levels of the proliferation marker Ki-67 in the transplanted tumours. Scale bar = 50 μm. (**E**) Schematic illustration of the mechanism by which *AP5Z1* influences apoptosis and autophagy in HCC cells (By Fig draw). The in vivo studies utilized a four-group design with 5 biologically independent animals per group, whereas the in vitro analyses included three separate experiments. The data are expressed as the means ± SEMs. Significance levels are denoted by * for $P < 0.05$, ** for $P < 0.01$, and *** for $P < 0.001$

autophagy can operate upstream of apoptosis to modulate its activity [42]. Our research demonstrated the same result: *AP5Z1* could affect the degree of apoptosis in cancer by regulating autophagy.

We further investigated the specific mechanism by which *AP5Z1* regulates autophagy and apoptosis in HCC cells. On the basis of our RNA-seq results, this gene may mediate many biological processes through the PI3K/Akt pathway. Since the AP-5 complex was discovered fairly recently, whether it is involved in the PI3K/Akt signalling pathway is unknown. However, depletion of its family member AP-2 inhibits agonist-induced internalization of protease-activated receptor 4 (PAR4), which can increase extracellular signal-regulated kinase 1/2 (ERK1/2) signalling and significantly reduce Akt signalling [43]. These findings suggest that AP-5 may be involved in regulating the Akt pathway. Through Co-IP assays, we validated the direct interaction between *AP5Z1* and PTEN. This interaction is important for tumour suppression mechanisms, given that PTEN is a critical tumour suppressor protein closely associated with the PI3K/Akt signalling pathway. PTEN primarily functions to inhibit this pathway by dephosphorylating phosphatidylinositol-3,4,5-trisphosphate (PIP3) via its lipid and protein phosphatase activities [44]. In our study, we found that AP5Z1 and PTEN expression were negatively correlated, suggesting that *AP5Z1* influences PI3K/Akt/mTOR signalling by modulating PTEN expression. Subsequent experiments revealed that both OE and KD of *AP5Z1* significantly altered the phosphorylation status of PI3K, Akt, and mTOR, while their total protein levels did not change. These findings suggest that *AP5Z1* modulates cellular signal transduction pathways by regulating the activities of key kinases, thereby influencing processes such as autophagy and apoptosis. Our rescue experiments provided additional confirmation of the mechanism by which *AP5Z1* modulates the PI3K/Akt/mTOR signalling pathway via PTEN, and these findings were further corroborated by the results of subsequent tumorigenesis experiments conducted in nude mice. Taken together, our findings suggest that the regulatory function of *AP5Z1* is contingent not only on its interaction with PTEN but also on extensive modulation of the PI3K/Akt/mTOR signalling pathway. We therefore propose that *AP5Z1* regulates this pathway via its association with PTEN in HCC cells to mediate autophagy and apoptosis.

E3 ubiquitin ligases play crucial roles in facilitating the ubiquitination of functional proteins to maintain protein homeostasis and stability. Aberrations in the ubiquitination regulation of key proteins can lead to persistent homeostatic imbalances within cells, potentially resulting in carcinogenesis [45, 46]. TRIM21 is part of the TRIM protein family, which has more than 80 members. These proteins feature several domains, such as the Really Interesting New Gene E3 ubiquitin ligase domain (RING), B-Box, and coiled-coil regions, at their N-termini. The *RING* domain of TRIM21 confers significant E3 ubiquitin ligase activity, which allows it to function by ubiquitinating substrate proteins [47–49]. TRIM proteins play pivotal roles in regulating various biological processes and diseases. TRIM21 has received considerable attention in cancer research in recent years; several studies have demonstrated that it can ubiquitinate claspin protein via K63-linked ubiquitin chains, leading to the inhibition of checkpoint kinase 1 (CHK1) activation and subsequently promoting tumour growth [50]. In HCC, TRIM21 functions as an oncogenic factor, facilitating both the initiation and progression of tumours [51, 52]. Our study revealed that *AP5Z1* OE in MHCC-97 H cells resulted in the ubiquitination and degradation of the PTEN protein via TRIM21, indicating that TRIM21 might play a key role as an E3 ligase in HCC regulation. Further experiments confirmed that TRIM21 interacted with both PTEN and *AP5Z1*, identifying PTEN as a substrate of TRIM21. By recruiting TRIM21, *AP5Z1* facilitates PTEN ubiquitination, which leads to the progression of HCC via the PI3K/Akt/mTOR pathway.

This study elucidated the potential application value of AP5Z1 in the diagnosis and treatment of hepatocellular carcinoma (HCC). These findings indicate that high expression of AP5Z1 can serve as a novel biomarker for prognostic evaluation in HCC patients, providing a crucial reference for the formulation of individualized treatment plans and survival prediction. Additionally, it offers new approaches for the diagnosis and treatment of HCC in the field of clinical laboratory science [53]. More importantly, targeted intervention strategies against AP5Z1 and its regulatory network (such as the development of specific small molecule inhibitors or gene editing therapies) may pave new avenues for precision medicine in HCC.

Despite the promising nature of these findings, we recognize several limitations in our current study, whose mediation is essential for the continuous advancement of scientific research and innovation [54]. First, the relatively small sample size, comprising only 60 pairs of clinical samples, may restrict the generalizability of our conclusions. Future research should aim to validate our findings through multicentre, large-sample cohort studies to increase the robustness and applicability of our results. Second, our mechanistic investigations have relied primarily on in vitro cell experiments and in vivo animal models. The biological functions of AP5Z1 in the human body, as well as its associated signalling pathways, require further validation through translational clinical research to bridge the gap between experimental and clinical settings. Third, although we elucidated the role of the AP5Z1–TRIM21–PTEN regulatory axis, our

understanding of the broader interaction protein network of AP5Z1 remains incomplete. Future studies could leverage high-throughput proteomics screening and bioinformatics analysis to systematically dissect its regulatory network, thereby providing a more comprehensive understanding of its biological significance.

Conclusions

In summary, our study demonstrated that the expression of *AP5Z1* was upregulated in hepatocellular carcinoma and was associated with a poor prognosis. As an oncogene, *AP5Z1* modulates the PI3K/Akt/mTOR pathway through its interaction with the PTEN protein, thereby influencing autophagy and apoptosis in HCC. PTEN was found to be a substrate of the E3 ubiquitin ligase TRIM21; *AP5Z1* could alter the level of ubiquitination of PTEN by recruiting TRIM21, which promoted its degradation. Accordingly, *AP5Z1* might be useful in the prognostication and diagnosis of HCC and could offer novel treatment strategies.

Abbreviations
HCC	Hepatocellular carcinoma
AP5Z1	Adaptor-related protein complex 5 subunit ζ1
PTEN	Phosphatase and tensin homolog deleted on chromosome ten
PI3K	Phosphoinositide 3-kinase
Akt	Protein kinase B
mTOR	Mammalian target of rapamycin pathway
TRIM21	Tripartite motif-containing protein 21
AP	Adaptor protein complex
TCGA	The Cancer Genome Atlas
TNM	Tumor–node–metastasis
3-MA	3-methyladenine
RAPA	Rapamycin
CHX	Cycloheximide
LAMP1	Lysosomal-associated membrane protein 1
GO	Gene Ontology
KEGG	Kyoto Encyclopedia of Genes and Genomes
CDK	Cyclin-Dependent Kinase

Supplementary Information

The online version contains supplementary material available at https://doi.org/10.1186/s12967-025-06537-9.

Supplementary Material 1: Supplementary Fig. 1: Validation of AP5Z1 KD and OE efficiency. (A, B) Quantitative RT–PCR detection of AP5Z1 expression levels in cells(SUN-449,LM3,MHCC-97 H) after transfection. (C) WB detection of AP5Z1 expression levels in cells(SUN-449,LM3,MHCC-97 H) after transfection. Results are shown as the mean±standard error (SE) based on three separate experiments. Significance levels are denoted by: * for $P < 0.05$, ** for $P < 0.01$, and *** for $P < 0.001$.

Supplementary Material 2: Supplementary Fig. 2: Investigation of the Link Between AP5Z1 and the PI3K/AKT Pathway. (A) Following AP5Z1 knockdown, 39 genes within the PI3K/AKT pathway showed differential expression.(B) Utilization of the TCGA database to assess the relationship between AP5Z1 and the PI3K/AKT signaling pathway(C) WB analysis was performed to examine the effects of AP5Z1 knockdown on the PI3K/Akt/mTOR signaling pathway in LM3 cells. Results are shown as the mean±standard error (SE) based on three separate experiments. Significance levels are denoted by: * for $P < 0.05$, ** for $P < 0.01$, and *** for $P < 0.001$.

Supplementary Material 3

Supplementary Material 4

Declarations

Ethics approval and consent to participate
The study was approved by the Committee on the Ethics of the First Affiliated Hospital of Guangxi Medical University (Approval number: 2024-E754-01) on October 24, 2024. Additionally, the animal experiments were approved by the Laboratory Animal Ethics Committee of Guangxi Medical University, with the ethics number: No. 202405005.

Consent for publication
Written informed consent for publication was obtained from all participants.

Completing interest
All authors declared no competing interest.

Author details
¹Division of Hepatobiliary Surgery, The First Affiliated Hospital of Guangxi Medical University, NO 6 Shuangyong Road, Nanning, Guangxi 530021, China
²Key Laboratory of Early Prevention and Treatment for Regional High Frequency Tumor (Guangxi Medical University, Ministry of Education, Nanning, Guangxi 530021, China
³Guangxi Key Laboratory of Immunology and Metabolism for Liver Diseases, Nanning, Guangxi 530021, China
⁴Department of Radiation Oncology, The First Affiliated Hospital of Guangxi Medical University, Nanning, Guangxi 530021, China

References
1. Siegel RL, Miller KD, Jemal A. Cancer statistics, 2019. CA Cancer J Clin. 2019;69:7–34.
2. Valery PC, Laversanne M, Clark PJ, Petrick JL, McGlynn KA, Bray F. Projections of primary liver cancer to 2030 in 30 countries worldwide. Hepatology. 2018;67:600–11.
3. Sun J, Zhou C, Zhao Y, Zhang X, Chen W, Zhou Q, Hu B, Gao D, Raatz L, Wang Z, et al. Quiescin sulfhydryl oxidase 1 promotes sorafenib-induced ferroptosis in hepatocellular carcinoma by driving EGFR endosomal trafficking and inhibiting NRF2 activation. Redox Biol. 2021;41:101942.
4. Du A, Li S, Zhou Y, Disoma C, Liao Y, Zhang Y, Chen Z, Yang Q, Liu P, Liu S, et al. M6A-mediated upregulation of circmdk promotes tumorigenesis and

acts as a nanotherapeutic target in hepatocellular carcinoma. Mol Cancer. 2022;21:109.

5. Li Y, Guo M, Qiu Y, Li M, Wu Y, Shen M, Wang Y, Zhang F, Shao J, Xu X, et al. Autophagy activation is required for N6-methyladenosine modification to regulate ferroptosis in hepatocellular carcinoma. Redox Biol. 2024;69:102971.

6. Aghapour SA, Torabizadeh M, Bahreiny SS, Saki N, Jalali Far MA, Yousefi-Avarvand A, Dost Mohammad Ghasemi K, Aghaei M, Abolhasani MM, Sharifani MS, et al. Investigating the dynamic interplay between cellular immunity and tumor cells in the fight against cancer: an updated comprehensive review %J. Iran J Blood Cancer. 2024;16:84–101.

7. Sanger A, Hirst J, Davies AK, Robinson MS. Adaptor protein complexes and disease at a glance. J Cell Sci. 2019;132.

8. Robinson MS. Adaptable adaptors for coated vesicles. Trends Cell Biol. 2004;14:167–74.

9. Hirst J, Itzhak DN, Antrobus R, Borner GHH, Robinson MS. Role of the AP-5 adaptor protein complex in late endosome-to-Golgi retrieval. PLoS Biol. 2018;16:e2004411.

10. Hoshi N, Uemura T, Tachibana K, Abe S, Murakami-Nishimagi Y, Okano M, Noda M, Saito K, Kono K, Ohtake T, Waguri S. Endosomal protein expression of gamma1-adaptin is associated with tumor growth activity and relapse-free survival in breast cancer. Breast Cancer. 2024;31:305–16.

11. Wu G, Chen M, Ren H, Sha X, He M, Ren K, Qi J, Lin F. AP3S1 is a novel prognostic biomarker and correlated with an immunosuppressive tumor microenvironment in Pan-Cancer. Front Cell Dev Biol. 2022;10:930933.

12. Kong D, Wu Y, Liu Q, Huang C, Wang T, Huang Z, Gao Y, Li Y, Guo H. Functional analysis and validation of Oncodrive gene AP3S1 in ovarian cancer through filtering of mutation data from whole-exome sequencing. Eur J Med Res. 2024;29:231.

13. Cho SH, Pak K, Jeong DC, Han ME, Oh SO, Kim YH. The AP2M1 gene expression is a promising biomarker for predicting survival of patients with hepatocellular carcinoma. J Cell Biochem. 2019;120:4140–6.

14. Pignatelli J, Jones MC, LaLonde DP, Turner CE. Beta2-adaptin binds actopaxin and regulates cell spreading, migration and matrix degradation. PLoS ONE. 2012;7:e46228.

15. Hirst J, Madeo M, Smets K, Edgar JR, Schols L, Li J, Yarrow A, Deconinck T, Baets J, Van Aken E, et al. Complicated spastic paraplegia in patients with AP5Z1 mutations (SPG48). Neurol Genet. 2016;2:e98.

16. Breza M, Hirst J, Chelban V, Banneau G, Tissier L, Kol B, Bourinaris T, Said SA, Péréon Y, Heinzmann A, et al. Expanding the spectrum of AP5Z1-Related hereditary spastic paraplegia (HSP-SPG48): A multicenter study on a rare disease. Mov Disord. 2021;36:1034–8.

17. Liu L, Michowski W, Kolodziejczyk A, Sicinski P. The cell cycle in stem cell proliferation, pluripotency and differentiation. Nat Cell Biol. 2019;21:1060–7.

18. Matthews HK, Bertoli C, de Bruin RAM. Cell cycle control in cancer. Nat Rev Mol Cell Biol. 2022;23:74–88.

19. Hume S, Dianov GL, Ramadan K. A unified model for the G1/S cell cycle transition. Nucleic Acids Res. 2020;48:12483–501.

20. Chu C, Geng Y, Zhou Y, Sicinski P. Cyclin E in normal physiology and disease States. Trends Cell Biol. 2021;31:732–46.

21. Hwang HC, Clurman BE. Cyclin E in normal and neoplastic cell cycles. Oncogene. 2005;24:2776–86.

22. Boice A, Bouchier-Hayes L. Targeting apoptotic caspases in cancer. Biochim Biophys Acta Mol Cell Res. 2020;1867:118688.

23. Hirst J, Edgar JR, Esteves T, Darios F, Madeo M, Chang J, Roda RH, Dürr A, Anheim M, Gellera C, et al. Loss of AP-5 results in accumulation of aberrant endolysosomes: defining a new type of lysosomal storage disease. Hum Mol Genet. 2015;24:4984–96.

24. Dossou AS, Basu A. The emerging roles of mTORC1 in macromanaging autophagy. Cancers (Basel). 2019;11.

25. Reymond A, Meroni G, Fantozzi A, Merla G, Cairo S, Luzi L, Riganelli D, Zanaria E, Messali S, Cainarca S, et al. The tripartite motif family identifies cell compartments. Embo J. 2001;20:2140–51.

26. Zaremba S, Keen JH. Assembly polypeptides from coated vesicles mediate reassembly of unique clathrin coats. J Cell Biol. 1983;97:1339–47.

27. Pearse BM, Robinson MS. Purification and properties of 100-kd proteins from coated vesicles and their reconstitution with clathrin. EMBO J. 1984;3:1951–7.

28. Robinson MS, Bonifacino JS. Adaptor-related proteins. Curr Opin Cell Biol. 2001;13:444–53.

29. Hirst J, Barlow LD, Francisco GC, Sahlender DA, Seaman MN, Dacks JB, Robinson MS. The fifth adaptor protein complex. PLoS Biol. 2011;9:e1001170.

30. Hirst J, Hesketh GG, Gingras AC, Robinson MS. Rag GTPases and phosphatidylinositol 3-phosphate mediate recruitment of the AP-5/SPG11/SPG15 complex. J Cell Biol. 2021;220.

31. Germic N, Frangez Z, Yousefi S, Simon HU. Regulation of the innate immune system by autophagy: neutrophils, eosinophils, mast cells, NK cells. Cell Death Differ. 2019;26:703–14.

32. Xia H, Green DR, Zou W. Autophagy in tumour immunity and therapy. Nat Rev Cancer. 2021;21:281–97.

33. Debnath J, Gammoh N, Ryan KM. Autophagy and autophagy-related pathways in cancer. Nat Rev Mol Cell Biol. 2023;24:560–75.

34. Onorati AV, Dyczynski M, Ojha R, Amaravadi RK. Targeting autophagy in cancer. Cancer. 2018;124:3307–18.

35. Amaravadi RK, Kimmelman AC, Debnath J. Targeting autophagy in cancer: recent advances and future directions. Cancer Discov. 2019;9:1167–81.

36. Diling C, Yinrui G, Longkai Q, Xiaocui T, Yadi L, Xin Y, Guoyan H, Ou S, Tianqiao Y, Dongdong W, et al. Circular RNA NF1-419 enhances autophagy to ameliorate senile dementia by binding Dynamin-1 and adaptor protein 2 B1 in AD-like mice. Aging. 2019;11:12002–31.

37. Carneiro BA, El-Deiry WS. Targeting apoptosis in cancer therapy. Nat Rev Clin Oncol. 2020;17:395–417.

38. Kaufmann SH, Earnshaw WC. Induction of apoptosis by cancer chemotherapy. Exp Cell Res. 2000;256:42–9.

39. Rajabi L, Ebrahimdoost M, Mohammadi SA, Soleimani Samarkhazan H, Khamisipour G, Aghaei M. Aqueous and ethanolic extracts of Moringa oleifera leaves induce selective cytotoxicity in Raji and Jurkat cell lines by activating the P21 pathway independent of P53. Mol Biol Rep. 2025;52:102.

40. Eisenberg-Lerner A, Bialik S, Simon HU, Kimchi A. Life and death partners: apoptosis, autophagy and the cross-talk between them. Cell Death Differ. 2009;16:966–75.

41. Scott RC, Juhász G, Neufeld TP. Direct induction of autophagy by Atg1 inhibits cell growth and induces apoptotic cell death. Curr Biol. 2007;17:1–11.

42. Bai Y, Liu X, Qi X, Liu X, Peng F, Li H, Fu H, Pei S, Chen L, Chi X, et al. PDIA6 modulates apoptosis and autophagy of non-small cell lung cancer cells via the MAP4K1/JNK signaling pathway. EBioMedicine. 2019;42:311–25.

43. Smith TH, Coronel LJ, Li JG, Dores MR, Nieman MT, Trejo J. Protease-activated Receptor-4 signaling and trafficking is regulated by the clathrin adaptor protein Complex-2 independent of beta-Arrestins. J Biol Chem. 2016;291:18453–64.

44. Carracedo A, Pandolfi PP. The PTEN-PI3K pathway: of feedbacks and cross-talks. Oncogene. 2008;27:5527–41.

45. Kumar S, Fairmichael C, Longley DB, Turkington RC. The multiple roles of the IAP Super-family in cancer. Pharmacol Ther. 2020;214:107610.

46. Humphreys LM, Smith P, Chen Z, Fouad S, D'Angiolella V. The role of E3 ubiquitin ligases in the development and progression of glioblastoma. Cell Death Differ. 2021;28:522–37.

47. Cappadocia L, Lima CD. Ubiquitin-like protein conjugation: structures, chemistry, and mechanism. Chem Rev. 2018;118:889–918.

48. Di Rienzo M, Romagnoli A, Antonioli M, Piacentini M, Fimia GM. TRIM proteins in autophagy: selective sensors in cell damage and innate immune responses. Cell Death Differ. 2020;27:887–902.

49. Hatakeyama S. TRIM family proteins: roles in autophagy, immunity, and carcinogenesis. Trends Biochem Sci. 2017;42:297–311.

50. Zhu X, Xue J, Jiang X, Gong Y, Gao C, Cao T, Li Q, Bai L, Li Y, Xu G, et al. TRIM21 suppresses CHK1 activation by preferentially targeting CLASPIN for K63-linked ubiquitination. Nucleic Acids Res. 2022;50:1517–30.

51. Wang Y, Sandrine IK, Ma L, Chen K, Chen X, Yu Y, Wang S, Xiao L, Li C, Liu Y, et al. TNKS1BP1 facilitates ubiquitination of CNOT4 by TRIM21 to promote hepatocellular carcinoma progression and immune evasion. Cell Death Dis. 2024;15:511.

52. Wang F, Zhang Y, Shen J, Yang B, Dai W, Yan J, Maimouni S, Daguplo HQ, Coppola S, Gao Y, et al. The ubiquitin E3 ligase TRIM21 promotes hepatocarcinogenesis by suppressing the p62-Keap1-Nrf2 antioxidant pathway. Cell Mol Gastroenterol Hepatol. 2021;11:1369–85.

53. Aghaei M, Khademi R, Bahreiny SS, Saki N. The need to Establish and recognize the field of clinical laboratory science (CLS) as an essential field in advancing clinical goals. Health Sci Rep. 2024;7:e70008.
54. Saki N, Haybar H, Aghaei M. Subject: motivation can be suppressed, but scientific ability cannot and should not be ignored. J Transl Med. 2023;21:520.

Publisher's note

Springer Nature remains neutral with regard to jurisdictional claims in published maps and institutional affiliations.